



Sustainable environment approach by the usage of ceramic pottery waste in geopolymer mortar

Z. Bayer Ozturk¹ · R. Cırık¹ · İ. İ. Atabey²

Received: 31 January 2023 / Revised: 25 March 2023 / Accepted: 14 April 2023 / Published online: 29 April 2023

© The Author(s) under exclusive licence to Iranian Society of Environmentalists (IRSEN) and Science and Research Branch, Islamic Azad University 2023

Abstract

This study aims to evaluate the pottery waste obtained from a pottery company in Cappadocia (Turkey) in the production of geopolymer mortars (GMs), which is becoming increasingly interesting in construction technology. For this purpose, mortars were prepared by replacing the fly ash with pottery wastes at proportions of 0%, 10%, 20%, 30%, and 40% by weight. Flow table, water absorption, apparent porosity, flexural strength, compressive strength, and high-temperature resistance tests were applied to GMs. Diopside, calcium silicate hydrate, and wollastonite crystals were observed in phase analyses performed by XRD for mortar containing 40% pottery waste. The observed microstructure analysis of before and after high-temperature tests was performed to investigate the effect of pottery waste on GMs. Consequently, better results were obtained at high-temperature strength up to 800 °C compared to the reference (0% pottery waste) by replacing up to 40% of fly ash with pottery waste to improve the physical and mechanical properties. Pottery waste replacement enhanced the flexural strength and compressive strength at 28 days by up to 26% and 64%, respectively, compared to reference mortar at ambient conditions. Furthermore, considering the overall mechanical and microstructural analysis, GMs with pottery waste promise sustainable mortar production and waste elimination. The pottery waste is a potential alternative material to be successfully recycled in the eco-friendly geopolymer mortars as a replacement of fly ash up to 40% level.

Keywords Pottery waste · Geopolymer · Strength · Microstructure · High temperature

Introduction

There has been a significant increase in consumption due to the growing population. In addition, the rise in industrial manufacturing also led to a surge in the generated hazardous/non-hazardous solid waste. Awareness has already been raised about the harm such solid wastes cause to both human health and the environment. Studies are carried out by researchers on the recycling of wastes and their usability as raw materials in a variety of fields (Khale and Chaudhary 2007; Zeybek 2009).

The construction sector produces vast quantities of greenhouse gas emissions during cement manufacturing. Considering the damage caused by such gas emissions on the environment, the usage of wastes in the manufacturing processes of geopolymer materials that are used in the production of materials resistant to heat and corrosive environmental conditions may contribute to the elimination of such problems (Alvarez-Ayuso et al. 2008; Atabey 2017; Maraş 2021). In terms of the environmental impact, and similar/higher mechanical-durability properties the most significant advantage of geopolymers in comparison with cement-based mortar is that geopolymer production releases much less CO₂. The reason for this is that there is no elevated temperature calcination phase during the geopolymer synthesis (Atabey 2017; Alomayri and Adesina 2021). Geopolymers are based on the formation of three-dimensional polymeric chains between Al–Si–O complexes as a result of the dissolution of wastes or by-products such as alumina and silica-rich metakaolin, fly ash, and ground blast furnace slag in an alkali solution (Arellano Aguilar et al. 2010; Robayo-Salazar and de Gutierrez 2018; Atabey and Bayer Ozturk 2021). The cost of fly ash which is one of the

Editorial responsibility: Jing Chen.

✉ Z. Bayer Ozturk
z.ozturk@nevsehir.edu.tr

¹ Department of Metallurgy and Materials Engineering, Nevsehir Haci Bektas Veli University, 50300 Nevsehir, Turkey

² Department of Civil Engineering, Nevsehir Haci Bektas Veli University, 50300 Nevsehir, Turkey



main materials used in the production of geopolymer concrete increased parallel to the value of the geopolymer due to the long distances to thermal power plants. Classified as waste, fly ash has become one of the main materials for the generation of geopolymer. Moreover, as fly ash may be used in the manufacturing of concrete, cement, aggregate, gas concrete, brick, road, and ground improvement applications, the cost of manufacturing increased, which led manufacturers to turn to different raw materials or solid waste materials (Kaplan and Gultekin 2010).

Pottery, including earthenware, stoneware, and porcelain, is a ceramic made from raw materials, such as clay, quartz, and feldspar, through densification at firing temperatures of 1000–1400 °C (Hao et al. 2022). It is possible to obtain products of various sizes by shaping the mud by hand or through a potter's wheel. Such products include earthenware bowls, pots, jugs, vases, jars, etc., with or without glazing. Pottery making continues in the Avanos district of Nevsehir province on the banks of the Kizilirmak river while carrying the traces of the past (avanospottery.com 2022). Avanos district of the Cappadocia region is predominantly known as the handicraft center of the region. In the pottery plant located in the said district, handmade jars, flower pots, press-printed products, indoor and outdoor ceramics shaped by casting and garden ceramics have been produced since 1998 (avanospottery.com 2022). Faulty products that are discarded at the furnace exit after production in the company form a large pile in the stock area and since their recycling to production is carried out to a very limited extent, they create a storage problem due to visual pollution as well as being kept as waste.

In the literature, the effects of using red clay ceramic powder (Keppert et al. 2018), fine waste dust from brick and roof tile production, red mud (Mucsi et al. 2019; Qaidi et al. 2022), ceramic tile waste (Reig et al. 2014; Huseien et al. 2019, 2020), and sanitaryware wastes (Atabey and Bayer Ozturk 2021; Bayer Ozturk and Atabey 2022) were investigated. In the studies carried out with ceramic wastes, it is seen that especially ceramic tiles/sanitaryware wastes have been the subject of research in geopolymers in the literature. But, we have not found any studies addressing the use of pottery wastes by the alkali activation method. This study investigated the effect of the usage of pottery wastes which are industrial wastes produced in Avanos-Cappadocia (Turkey) in geopolymers produced with fly ash on the geopolymer strengths, phase, and microstructure.

Materials and methods

Materials

Pottery wastes, fly ash, river sand, sodium hydroxide and tap water were used to produce geopolymer mortars

(GMs). The pottery wastes for the geopolymer mixtures were obtained from Anadolu Pottery (Avanos/Nevşehir). The wastes obtained from the company as post-fired shards were exposed to a grinding process in the ring mill of BC Teknoloji (Nevşehir) company to pass through a 63- μm sieve. The specific gravity of the F fly ash taken from the Sugözü/Turkey thermal power plant is 2.30, and its residue on 45 μm sieve is 20%. Sieve analysis values of sand are presented in Fig. 1. The pottery ceramic wastes preparation process in the factory and preparation of pottery waste-based mortars are shown in Fig. 2. Bulk specific gravity saturated surface dry of river sand is 2.67, and water absorption rate is 1.94 (TS EN 1097-6). The purity of sodium hydroxide used as an activator is 98.3%. Potable tap water was used in the mixtures (TS EN 1008). Discarded pottery wastes were supplied from Anadolu Pottery (Avanos-Turkey) company and were ground in a ring mill and sieved through a 63-micron sieve. The chemical analysis of pottery waste and fly ash was performed by using X-ray fluorescence analyses (XRF, Rigaku ZSX spectrometer) and is given in Table 1. The total $\text{SiO}_2 + \text{Al}_2\text{O}_3$ ratio in chemical contents was shown as 70% and 82% for pottery waste and fly ash, respectively. The CaO ratio of pottery waste was found as 16.31%. The X-ray diffraction analysis of pottery waste is demonstrated in Fig. 3. The phases obtained from the waste are quartz (SiO_2), microcline (KAlSi_3O_8) and diopside ($\text{Mg}_{0.964}\text{Fe}_{0.036}$) ($\text{Ca}_{0.94}\text{Na}_{0.06}$) Si_2O_6 .

Mix design and experimental method

The mortars' ratio of liquid/powder (Powder: fly ash + pottery wastes) in the mortars was determined as 0.40, and the sand/powder ratio was 3. Sodium hydroxide (NaOH) was used at 12 M (87 g) as an activator. The amounts of materials used to prepare the mixture are presented in Table 2. The first mixture in which fly ash was used as 450 g was taken as the reference (0% pottery) and new mixtures were

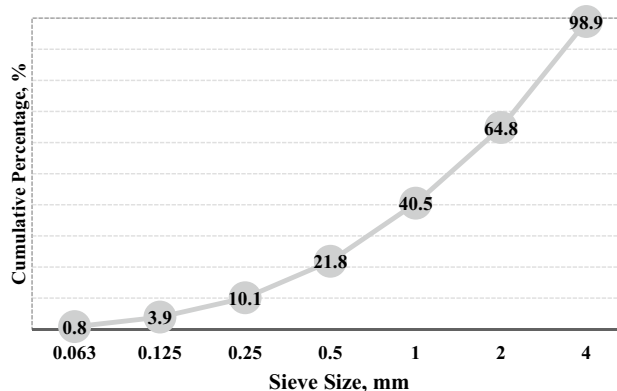


Fig. 1 Sieve analysis of sand



Fig. 2 Preparation of pottery waste and production of mortar from pottery waste and fly ash

Table 1 Chemical analysis of pottery waste and fly ash (%)

Oxide	SiO ₂	Al ₂ O ₃	Fe ₂ O ₃	CaO	MgO	SO ₃	Na ₂ O	K ₂ O	TiO ₂	MnO	SiO ₂ /Al ₂ O ₃
Fly ash	60.51	21.69	7.85	1.52	1.65	0.53	0.92	2.58	–	–	2.78
Pottery waste	54.46	15.77	3.51	16.31	3.04	0.37	1.25	3.26	0.66	0.0	3.45

Fig. 3 XRD phase analysis of pottery waste

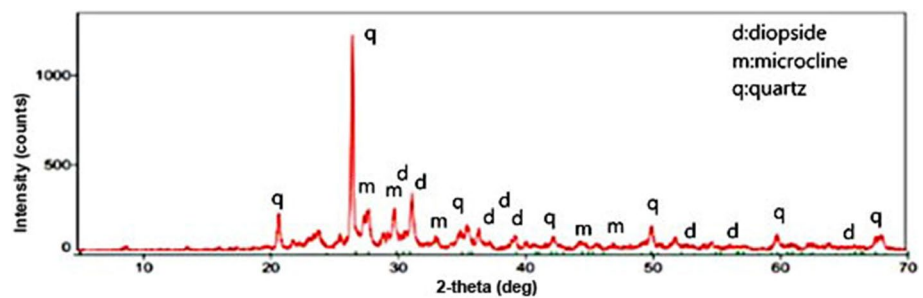


Table 2 Mixture proportions of mortars

Mixtures	Fly ash, g	Pottery waste, g	Sand, g	NaOH, g	Water, g
M0	450	–	1350	87	180
M10	405	45	1350	87	180
M20	360	90	1350	87	180
M30	315	135	1350	87	180
M40	270	180	1350	87	180

prepared by adding 10%, 20%, 30%, 40%, and 50% pottery waste instead of fly ash. In order to prepare the solution, water and NaOH were added to glass jars and the chemical was dissolved completely by shaking for about 1 min. Since the reaction of sodium hydroxide with water was exothermic, it was kept at room temperature until it cooled down to that point. Using these solutions at room temperature, mortar samples of 40 × 40 × 160 mm³ were produced according to TS EN 196-1 standard (EN 196-1). A Hobart-type mixer was used in the preparation of the mortar mix. Solution and powder wastes were first placed in the mixing bowl and mixed for 30 s (140 rpm), and then, sand was added within the second 30 s (140 rpm). Mixing was then continued at high speed (280 rpm) for another 30 s. The mixer was stopped,

the mortar on the walls of the container was collected in the middle in the first 30 s, and it waited for a total of 90 s. Then, the mixing process was completed by continuing at high speed for another 60 s.

M0 (0% pottery waste) was determined with only fly ash to study the effect of pottery waste ratio, curing time, and elevated temperature on the geopolymer mortar and this mix was pointed out as a control sample (reference). The code of mixes was determined based on varying pottery waste amounts in the geopolymer sample. For example, M10 represents replacing 10% of fly ash by pottery waste.

The flow table test was carried out on the mortars in accordance with the TS EN 1015-3 standard (TS EN 1015-3) when they were still fresh. Next, the mixtures were poured into mortar molds containing 3 chambers of 40 × 40 × 160 mm³. The mixtures poured into the 3-chamber mortar molds were then placed in an oven while still in their molds and were subjected to heat-curing at 90 °C for 24 h. Following the heat-curing process, mortar samples that were removed from their molds were kept in laboratory conditions at a temperature of approximately 23 ± 2 °C at 28 days. Then, unit weights, water absorption and apparent porosity of the samples were determined. Water absorption and porosity tests of geopolymer samples were measured

after curing at 90 °C for 24 h. After the curing times were completed, the mortar samples were taken from the oven and cooled to room temperature. Then, the water absorption and porosity values of the samples were measured according to (ASTM C642-06) at 28 days. Flexural (FS) and compressive strength (CS) tests were carried out on the samples in accordance with the TS EN 1015-11 standard (TS EN 1015-11) at 28 days. Each experimental value was found by averaging the results from 3 samples.

The samples produced to investigate the effects of elevated temperature were subjected to heat-curing for 24 h and were then kept at room temperature for 28 days. At the end of 28 days, samples were subjected to high temperature of 400 °C, 600 °C, and 800 °C for 60 min with a temperature increase of 5 °C/min, and the samples were left to cool down slowly for 24 h. An electric furnace (Carbolite CWF1200) was used for the high-temperature test. Microstructure examinations were also carried out using a scanning electron microscope (SEM, Zeiss Gemini 500) to investigate how the geopolymer samples prepared with the addition of pottery waste instead of fly ash affected the crystal formation and morphology change in internal structures. The samples taken for microstructural examination were coated with gold with the intent of capturing better display.

Results and discussion

Workability test was conducted on the GMs in the experimental study, while they were fresh. Unit weight, apparent porosity, water absorption, flexural strength, compressive strength, and elevated temperature tests were carried out on the hardened samples. In addition, SEM and XRD analyses were carried out for microstructure investigations. The

findings obtained at the end of the experimental study are given below;

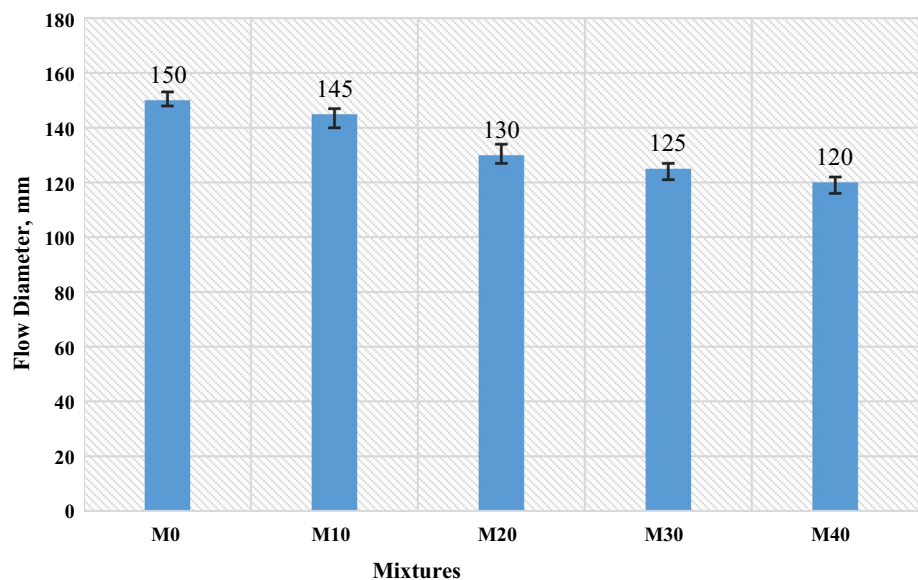
Flow table test

Flow table test values of mortars produced in this study are shown in Fig. 4. Workability test values of fresh mortar samples were in the range of 150–111 mm. Workability values decreased in comparison with a rise in the amount of pottery waste added instead of fly ash. In the preliminary trials, the workability value of the 50% pottery waste-added mortar was obtained as 111 mm. It has been determined that a maximum of 40% pottery waste can be added as the mortars have difficulty settling into the mold. Thus, measurements have been evaluated up to 40% for mortars, as mortar poses a problem in filling and consistency of the mold. In the previous studies, the specific surface area, grain shape, activator ratio and high CaO content and the development of the reaction rate and the formation of the C–A–S–H gel have been shown as factors affecting the workability (Liew et al. 2017; Shilar et al. 2022). It is thought that the workability values of the mortars, which are prepared with the increasing addition of pottery wastes, which have a higher CaO content (Table 1) compared to fly ash, improve the reaction rate, and their workability values decrease.

Water absorption and apparent porosity

Figure 5 shows the results of water absorption and apparent porosity tests conducted for the samples. The water absorption ratio of the GMs was calculated in the range of 8.4% and 7.8% and the apparent porosity in the range of 16.4% and 15.2%. With the increase in the amount of pottery waste, we found that the apparent porosity and

Fig. 4 Flow table test results of mortars



water absorption amount of the samples generally showed a trend of decrease compared to the M0. This result points to the fact that a dense structure was produced thanks to the reaction of crystals that may be formed due to CaO in waste with C–A–S–H gel in mortars activated with GMs with pottery waste. In addition, the water absorption of mortars is indirectly related to pore connectivity and volume. Ismail et al. (2014) stated that the C–A–S–H gel has a less porous structure than the N–A–S–H gel, which is the main reaction product occurring in the alkali-activated fly ash system (Ismail et al. 2014). When water absorption and porosity results of the samples were correlated with the compressive strength, the results were found to support each other (Fig. 7). In the previous studies, it was seen that the increase in the compressive strength of geopolymer mortars decreases the water absorption and porosity value (Thockhom et al. 2009; Jeyasehar et al. 2013).

Flexural strength

The changes in the flexural strength of the produced samples are shown in Fig. 6. While the FS of the reference specimen (M0) was found as 5.8 MPa at 28 days, the range of FS values of other samples (M10–M40) was obtained as 6.2–7.3 MPa along with the increase in the amount of pottery waste added. The GMs containing 40% pottery waste (M40) achieved the highest FS value (7.3 MPa) in 28 days. This value is 26% higher than the reference sample (M0). This result indicates that the appropriate amount of pottery waste substitution contributes to the flexural strength development of GMs. Pottery waste replacement positively affected the FS in all curing times (1, 7, and 28 days). The reason for this is believed to be the higher CaO amount in the pottery waste compared to fly ash ($\text{CaO}_{\text{waste}} 16.31 > \text{CaO}_{\text{UK}}$

1.52) (Table 2). It was observed in the literature that the flexural strength of samples rose to higher values due to the bond structure and bonding characteristics of CaO (Yip et al. 2008; Chindaprasirt et al. 2018). Moreover, when CaO from a calcium-rich raw material reacts with water, it generates heat from the exothermic process at ambient temperatures, and this created heat accelerates the reaction rate. Ca in the gel structure is also important in forming C–A–S–H and N–A–S–H alkaline-activated gels, and calcium has a positive contribution to the development of strength. This way the formation of reaction products is also affected by the accelerated reaction in fly ash-based geopolymers, and the mechanical strengths are thus improved (Chindaprasirt et al. 2018; Vafaei and Allahverdi 2006; Temuujin et al. 2009; Pangdaeng et al. 2014). The literature stated that there are two types of alkali aluminosilicate gel: Al-rich and Si-rich gel. The interaction between the Al-rich gel and the unreacted fly ash particles causes more microcracks to form in the gel matrix, reducing the strength (Fernandez-Jimenez et al. 2006). As the Si/Al ratio in the mixture increases, the flexural strength of the mortars will increase thanks to the good bonding between the geopolymer mortar and the aggregate, and the strong Si–O–Si interaction (Shilar et al. 2022). It is seen that the increasing Si/Al ratio (Fig. 6) due to the increase in the amount of pottery waste affects the flexural strength.

Compressive strength

The compressive strengths of the GMs are also shown in Fig. 7. As was the case in the flexural strength results, an increase in the compressive strength was established in line with the increase in the amount of the added pottery waste instead of fly ash. While the CS was 20.1 MPa at

Fig. 5 Water absorption and apparent porosity of mortars

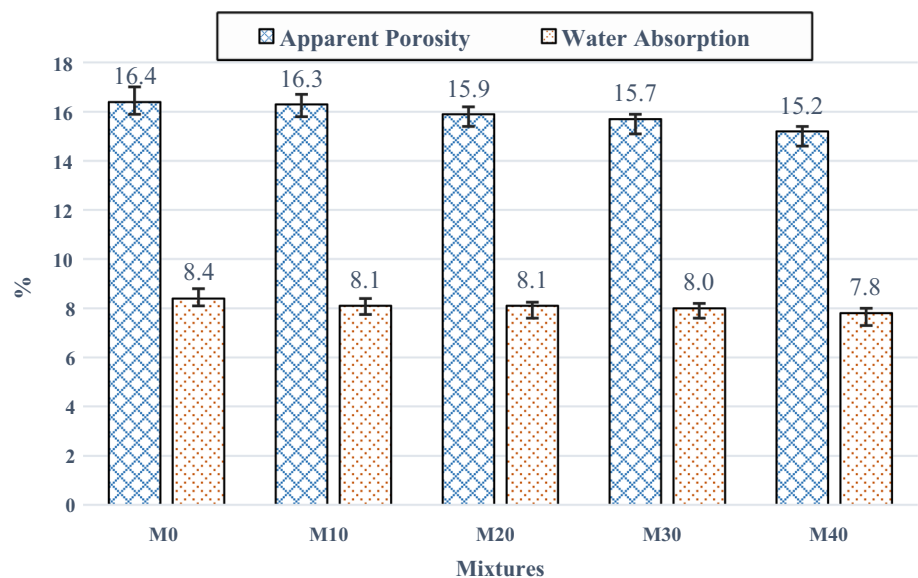


Fig. 6 1-day, 7-day, and 28-day flexural strength of GMs

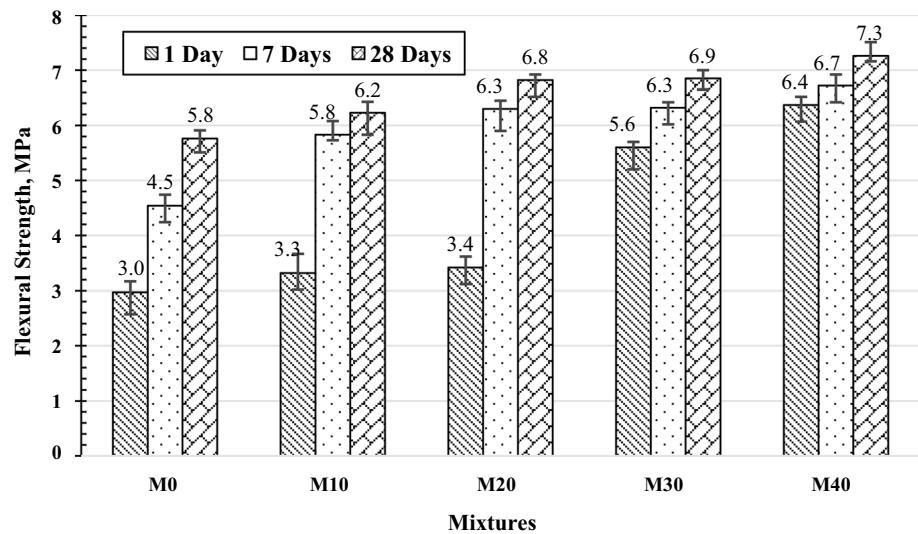
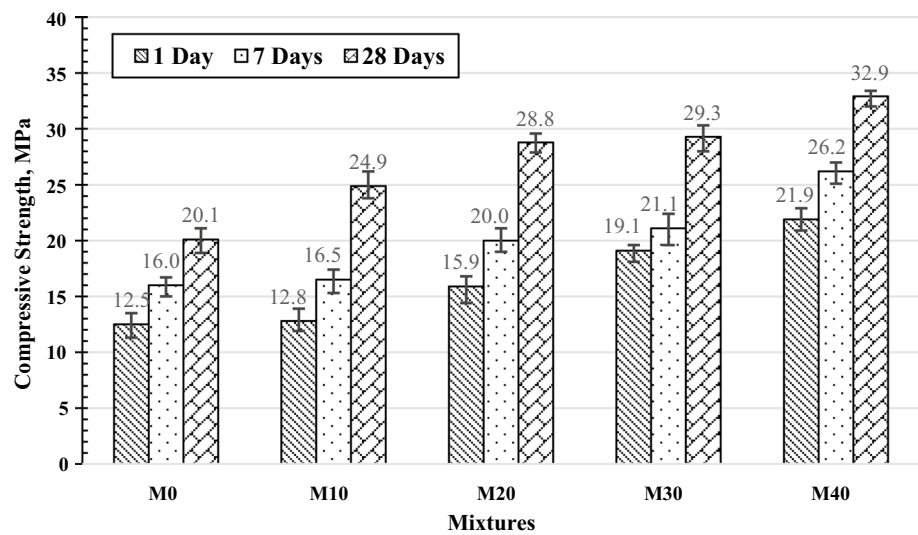


Fig. 7 1-day, 7-day, and 28-day compressive strength of GMs



28 days for the M0, the range of compressive strengths was found as in the range of 24.9 and 32.9 MPa for other samples (M10–M40). While the compressive strength of the reference specimen at 7 days was found as 16.0, the CS of the M40 specimen reached 26.2, an increase of approximately 64%. Otherwise, the compressive strength of the GMs gradually increased with the pottery waste ratio and reached its highest value at the 40% replacement level (M40) in all curing times. For instance, at room temperature, the compressive strength of specimens prepared with 10%, 20%, 30% and 40% pottery waste raised by 24%, 43%, 46%, and 64% at 28 days, respectively, as compared to that of the M0. The highest CS was 29.3 and 32.9 MPa, respectively, for the M30 and M40 for 28 days. The literature states that the CaO content increases the strength of geopolymers and that the CaO content has a significant effect on the formation of N(C)–A–S–H gels (Chindaprasirt et al. 2018; Pimraksa

et al. 2009; Kaya 2020). For this reason, it is thought that the increasing CaO content in the content due to the increase in pottery waste had a positive effect on the strength (Lee and Kang 2016). The improvement of CS by the inclusion of pottery waste can be attributed to the ability of the dense alumina silicate gel structure to fill the voids by accelerating the geopolymerization reaction.

Elevated temperature exposure

The flexural and compressive strength values after being subjected to elevated temperature are presented in Figs. 8 and 9, respectively. It was determined that the flexural and compressive strength values of all the samples exposed to 400 °C, 600 °C, and 800 °C temperatures were reduced. The test results demonstrated that each temperature range had a distinct pattern of strength loss. Higher strength results were

obtained in the samples containing pottery waste compared to the reference specimen. In the samples in which 40% pottery waste was used, the strength values reached higher levels more than twice the value obtained for the reference specimen at all three temperatures.

It is reported that the microstructure is affected by high temperature and the formation of micro cracks is the reason for the decrease in the flexural strength under the influence of temperature in the literature (Saridemir et al. 2020). Additionally, the factor affecting the strength is microstructural development (acicular crystals such as wollastonite, dense microstructure) as well as porosity. While the flexural strength of the M0 at 400 °C is 1.2 MPa, the range of FS observed in the samples containing pottery waste was from 1.9 to 3.4 MPa depending on the amount of waste increase. For the reference sample, the flexural strength was observed as 1.0 MPa at 600 °C and higher FS was observed from 1.2

to 3.2 MPa for the samples containing pottery waste. At 800 °C, the flexural strength value of the reference mortar reduced from 5.8 to 0.4 MPa with respect to their unheated (25 °C) atmosphere. The reductions in the flexural strength values of pottery waste incorporated GMs varied from 0.6 to 1.5 MPa.

With the increase in the amount of pottery waste, higher compressive strength was obtained in the mortars exposed to high temperatures compared to the reference samples. For example, while the CS values of M0 mortar at 400, 600 and 800 °C were 9.9, 8.7, and 5.6 MPa, these values were obtained for the M40 sample as 18.4, 19.5, and 19.7. (Fig. 9). An increase in SiO₂/Al₂O₃ ratio may be responsible for the augments in compressive strength due to Si–O–Si bonds, which are more potent than Si–O–Al bonds (Duxcon et al. 2007; Ozer and Soyer Uzun 2015; Lahoti et al. 2017). In previous studies, the usage of Ca-rich materials in

Fig. 8 Flexural strength of GMs at ambient and elevated temperatures

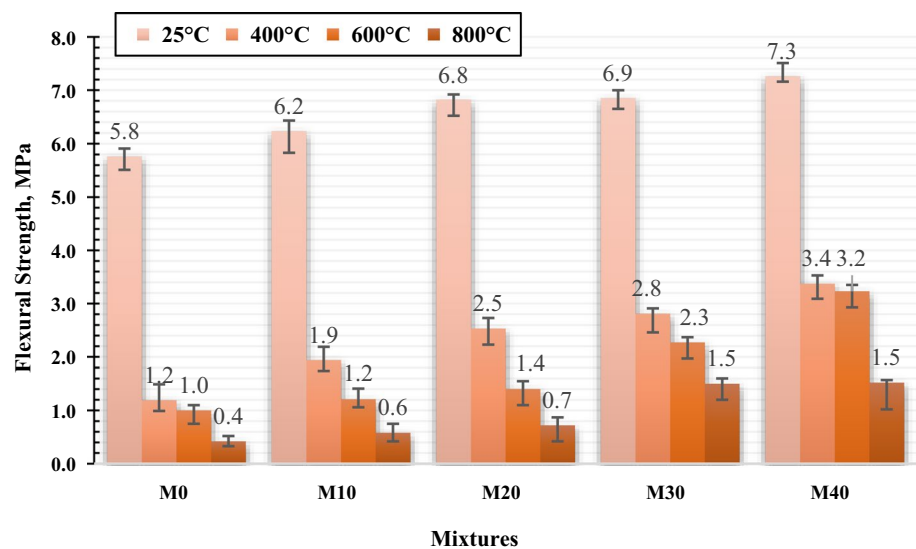
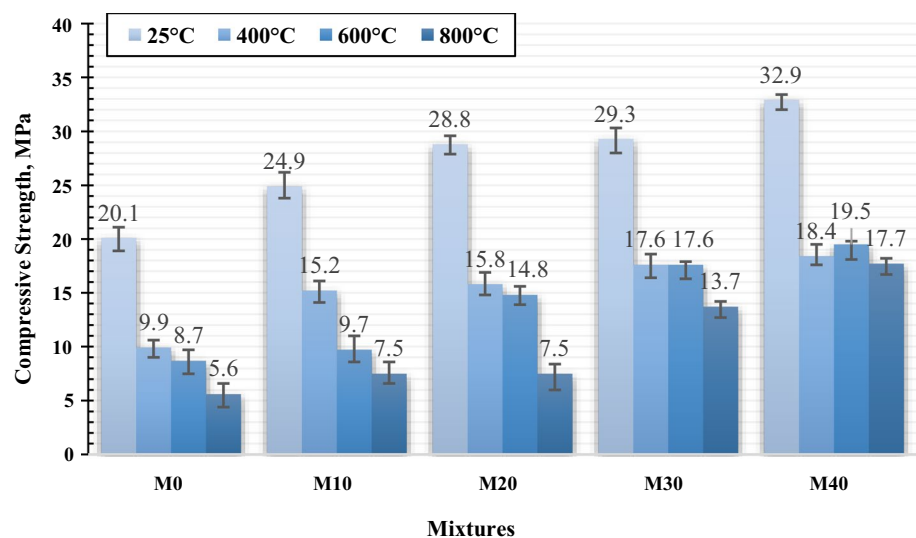


Fig. 9 Compressive strength of GMs at ambient and elevated temperatures



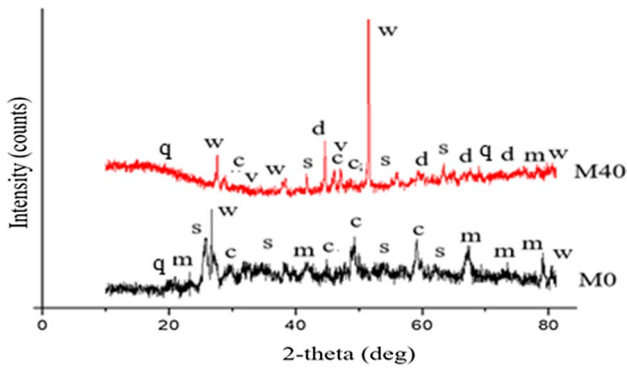


Fig. 10 XRD patterns of M0 and M40 samples (*W* wollastonite, *d* diopside, *v* vermiculite, *s* sodium aluminum silicate hydrate, *c* calcium silicate hydrate, *m* microsommitte)

geopolymer mortars has been reported to improve strengths (Yip et al. 2008; Bernal et al. 2011; Qian and Song 2015; Payne et al. 2017). Accordingly, it is thought that both the high Si/Al ratio and CaO content of the samples containing pottery wastes increased the CS values compared to

the reference at elevated temperatures (Davidovits 1989). The SEM analyses (Figs. 11, 12 and 13) were employed to explain the strength and microstructure relationship and the formation of wollastonite, diopside and calcium silicate hydrate crystals. It stated that the toughening effects of wollastonite usage result from the needle-like form of wollastonite that significantly bridge cracks at the micro-level in previous studies. Thus, it delays microcrack coalescence and increases strength (Dutkiewich et al. 2022).

Phase and microstructure analysis

The phases of M0 and M40 samples are shown in Fig. 10. The crystalline phases were identified as diopside, quartz, and vermiculite ($\text{Na-K-Al-O-Si } 12\text{H}_2\text{O}$) derived from pottery waste, additionally wollastonite (CaSiO_3), calcium silicate hydrate was formed depending on a high amount of Ca content in pottery waste. Sharp-high peaks (especially wollastonite) indicate the referential growth in the M40 sample. Microsommitte ($\text{Na}_4\text{K}_2\text{Ca}_2(\text{AlSiO}_4)_6\text{ClSO}_4$), calcium silicate hydrate, and sodium aluminum silicate

Fig. 11 SEM images of M0 **a** before elevated temperatures (25 °C), **b** at 400 °C, **c** at 600 °C

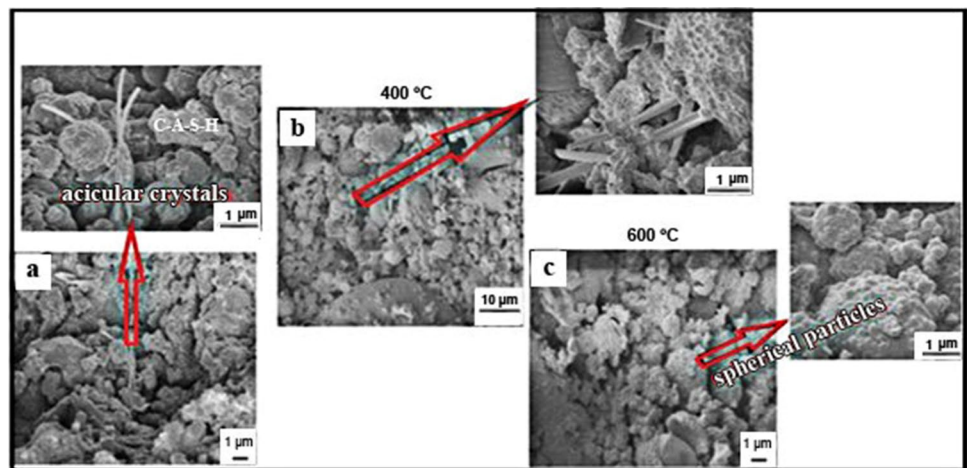


Fig. 12 SEM images of M10 **a** before elevated temperature, (25 °C), **b** at 400 °C

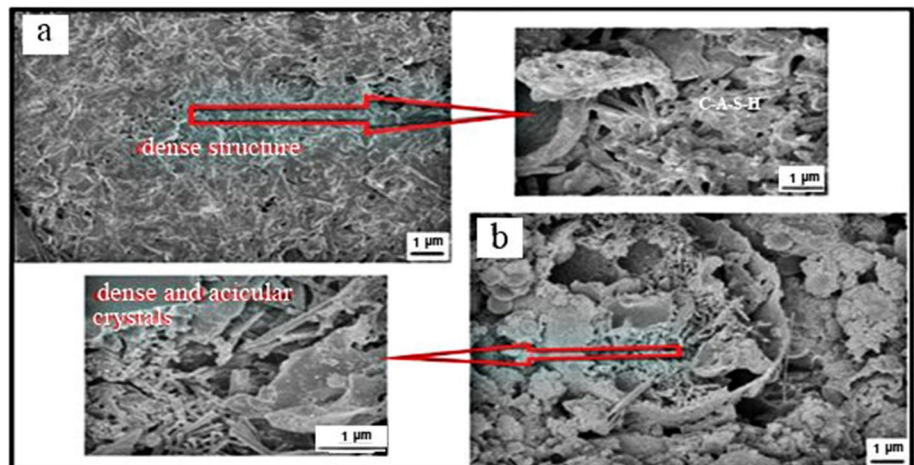
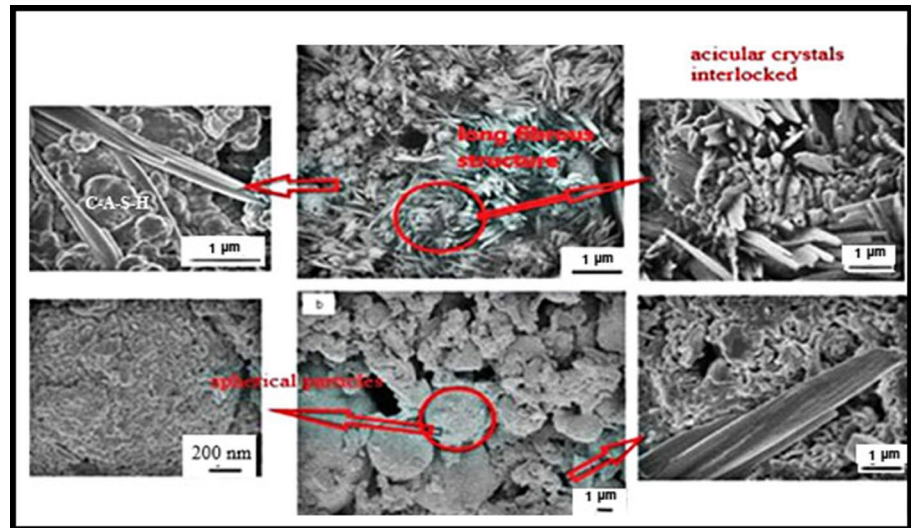


Fig. 13 SEM images of M40 **a** before elevated temperature, **b** at 400 °C



hydrate ($\text{Na}_4\text{Al}_2\text{Si}_6\text{O}_{17}2\text{H}_2\text{O}$) were formed in the M0 sample. After the displacement of fly ash and pottery waste (from M0 to M40), the peak of sodium aluminum silicate hydrate was reduced, wherein the peaks of wollastonite, calcium silicate hydrate, and diopside became progressively stronger. Raising the Ca amount caused a more compact and finer microstructure indicating that calcium is acting as a seeding or precipitating element. Several studies stated that calcium-containing compounds were formed by the interaction of the calcium hydroxide with dissolved aluminosilicates or sodium silicate solution. The probable reaction products would be calcium silicate hydrate (C S H) or calcium aluminosilicate either in amorphous or poorly ordered crystalline form which would be difficult to detect by XRD (Temujin et al. 2009). Therefore, the wollastonite observed and calcium silicate hydrate peak intensities exhibited an increase compared to M0. Additional calcium released from the pottery waste reacts rapidly with Si and Al to form the geopolymeric gel and this may have formed wollastonite crystals.

Sample microstructures at 400 °C and 600 °C were investigated before and after elevated temperatures on the M0 specimens. Upon further examination of general and magnified images of the sample microstructures, we observed following the increase in temperatures that a few fibrous crystals were observed at 400 °C before and after elevated temperatures, and however, they disappeared at 600 °C (Fig. 11). It is observed that acicular crystals disappear, and spherical particle agglomerations of 0.5-micron form at 600 °C. Calcium alumina silicate hydrate (CASH) spherical formations were found in images, but we found that these structures did not make a considerable contribution to the condensation due to the increase in temperature and that the porosity increased. This explains the decreases in strength

arising from temperature increase in the reference specimen (Fig. 11).

Microstructures of the samples of pottery wastes were included in the highest and lowest ratios instead of fly ash were compared. It is thought that especially with the increase in pottery waste from 10 to 40%, the large and numerous acicular crystals that develop due to the high CaO and $\text{SiO}_2/\text{Al}_2\text{O}_3$ content in the pottery waste compared to the fly ash in its composition, interlock with each other and improved the strength of mortars. The changes in the general and magnified microstructures of the samples before elevated temperature and after firing at 400 °C were investigated (Figs. 12 and 13). When examining the image of the M10 specimen before elevated temperature, we found that the structure was in the dense alumina silicate gel structure in the image given with small magnification, and acicular crystals (wollastonite) began to form in the enlarged images. When examined the microstructure of the M10 specimen at 400 °C, it was observed that acicular crystals became evident because of temperature, and crystals larger than 1 μm were formed. With the rise in the Ca/Si ratio, the morphology of the calcium silicate hydrate gel, a product of hydration, transforms from a thin sheet to a long fibrous structure (Chen et al. 2022). This proves how long fibrous crystals (wollastonite) and calcium silicate hydrate were formed in the M10 specimen with the high CaO from the pottery waste compared to the reference specimen and with the reduced SiO_2 content compared to the fly ash. We found that these long fibrous crystals tend to exhibit a compact structure and the alumina silicate gel can fill the voids and contribute to obtaining a dense structure. This may also explain the rise in strength values and decrease in water absorption in samples containing pottery waste before and after elevated temperature.

When examining the microstructure of the M40 specimen containing 40% pottery waste before elevated temperature,

we established that the long acicular crystals became more pronounced and reached 10 μm in size and formed a compact structure by interlocking (Fig. 13a). The reason why these acicular crystals became more pronounced was the high amount of CaO in the pottery waste. Following the addition of 40% pottery waste, the amount of CaO in the structure increased even more compared to the reference. This difference is evident in the enlarged versions of the microstructures. The acicular shape of wollastonite may overlap between each other and form network structures that can resist the flow of the mixture (Bong et al. 2020). In addition, with the increase in the Ca/Si ratio, the morphology of the calcium silicate hydrate gel, which is the hydration product, transforms from thin sheet to long fibrous structure (wollastonite crystals) and the compressive strength values increase in recent studies (Timakul et al. 2016; Bong et al. 2020). Upon exposure to high temperature at 400 °C, the (C, N)–A–S–H gel structure and needle-like crystals that began to dissolve in between were observed. It is noteworthy that the observed needle-like crystals before high temperature were disappear at 400 °C, and the presence of an amorphous structure containing round crystals in the markings with round (Fig. 13b).

Conclusion

- Replacing fly ash with pottery waste by up to 40% led to decreasing the flow table diameter. However, the GMs made by replacing 10% had a similar value to the M0.
- The addition of pottery waste reduced the void ratio, and accordingly, a slight decrease was observed in the water absorption ratio.
- The addition of pottery waste increased the flexural strength values compared to the reference (before the fire). M40 mortars compared to M0 have 26% higher flexural strength at 28 days.
- Regarding the mortar containing pottery waste, 40% was found to be the most effective level of substitution to improve the compressive strength during all curing period.
- The substitution of pottery waste for fly ash in GMs increased the high-temperature resistance.
- The strengths of the samples were continuously decreased with rising the temperature up to 800 °C. However, pottery waste-based mortars decreased at a lower rate compared to the control group.
- In phase and microstructure examinations of the samples, wollastonite, calcium aluminum silicate hydrate, and sodium aluminum silicate hydrate crystals were observed. It was observed that long fibrous wollastonite crystals became more pronounced as they formed a compact structure by interlocking at 400 °C for M40. The reason why crystals became more pronounced is the high CaO content in pottery waste.
- With the use of pottery waste up to 40% instead of fly ash in the manufacturing of geopolymer, the obtained values in the mechanical properties were more than higher than the reference sample. In addition to the mechanical tests of the obtained geopolymer mortar, the production cost and environmental impact also have a significant effect on the determination of the optimal pottery waste content. Technically, economically and ecologically optimum pottery waste level was found to be 40% by weight in fly ash-based geopolymers. High pottery waste usage will paramountly contribute to the waste recycling in the pottery industry.

Acknowledgements This work was supported by the Scientific and Research Projects of Nevsehir Hacı Bektaş Veli University (No: ABAP20F39). Pottery wastes were supported by the Anadolu Pottery Company (Nevsehir). The authors thank to NEVU and Anadolu Pottery.

Author contribution All authors contributed to the study conception and design. Material preparation, data collection and analysis were performed by ZBO, RC. ZBO contributed to conceptualization, investigation, methodology, data curation, writing—original draft, writing—review, editing, validation, and supervision. ZBO, RC and IIA contributed to methodology, investigation, and resources, writing—original draft.

Funding The authors declare that no funds, grants or other supports were received during the preparation of this manuscript.

Data availability Not applicable.

Declarations

Conflict of interest The authors declare that they have no conflict of interest.

References

- Alomayri TS, Adesina A (2021) The influence of nano CaCO_3 on the mechanical performance of micro glass-reinforced geopolymer paste. *Arab J Geosci* 14:14. <https://doi.org/10.1007/s12517-021-07839-0>
- Alvarez-Ayuso E, Querol X, Plana F et al (2008) Environmental, physical and structural characterisation of geopolymer matrix synthesised from coal (co-) combustion fly ashes. *J Hazard Mater* 154:175–183. <https://doi.org/10.1016/j.jhazmat.2007.10.008>
- Arellano Aguilar R, Burciaga Díaz O, Escalante García JI (2010) Lightweight concretes of activated metakaolin–fly ash binders, with blast furnace slag aggregates. *Const Build Mater* 24:1166–1175. <https://doi.org/10.1016/j.conbuildmat.2009.12.024>
- ASTM C642–06 (2013) Standard test method for density, absorption, and voids in hardened concrete. Annual book of ASTM Standards
- Atabey İİ (2017) Investigation of durability properties of F class fly ash geopolymer mortar. Doctorate thesis, Erciyes University, Kayseri Turkey



- Atabey İİ, Bayer Öztürk Z (2021) Investigation of usability of ceramic sanitaryware wastes in geopolymer mortar production. *IJ Eng Res Dev* 13:212–219. <https://doi.org/10.29137/umagd.782733>
- Avanos pottery (2022). <http://www.avanospottery.com/tr/>
- Bayer Öztürk Z, Atabey İİ (2022) Mechanical and microstructural characteristics of geopolymer mortars at high temperatures produced with ceramic sanitaryware waste. *Ceram Int* 48:12932–12944. <https://doi.org/10.1016/j.ceramint.2022.01.166>
- Bernal SA, Rodriguez ED, Gutierrez M et al (2011) Mechanical and thermal characterisation of geopolymers based on silicate-activated metakolin/slag blends. *J Mater Sci* 46:5477–5486. <https://doi.org/10.1007/s10853-011-5490-z>
- Bong SH, Nematollahi B, Xia M et al (2020) Properties of one-part geopolymer incorporating wollastonite as partial replacement of geopolymer precursor or sand. *Mater Lett* 263:127236. <https://doi.org/10.1016/j.matlet.2019.127236>
- Chen X, Zhan J, Lu M et al (2022) Study on the effect of calcium and sulfur content on the properties of fly ash based geopolymer. *Constr Build Mater* 314:125650. <https://doi.org/10.1016/j.conbuildmat.2021.125650>
- Chindaprasirt P, Phoo-ngernkham T, Hanjitsuwan S et al (2018) Effect of calcium-rich compounds on setting time and strength development of alkali-activated fly ash cured at ambient temperature. *Case Stud Constr Mater* 9:e00198. <https://doi.org/10.1016/j.cscm.2018.e00198>
- Davidovits J (1989) Geopolymers and geopolymeric new material. *J Therm Anal* 35:429–441
- Dutkiewich M, Yucel HE, Yıldızhan F (2022) Evaluation of the performance of different types of fibrous concretes produced by using wollastonite. *Materials* 15:6904. <https://doi.org/10.3390/ma15196904>
- Duxcon P, Fernandez-Jimenez A, Provis JL et al (2007) Geopolymer technology: the current state of the art. *J Mater Sci* 42:2917–2933. <https://doi.org/10.1007/s10853-006-0637-z>
- EN 196-1 (2016) Methods of testing cement—part 1: determination of strength. European Committee for Standardization (CEN), Brussels, Belgium
- Fernandez-Jimenez AM, Palomo A, Sobrados J, Sanz J (2006) The role played by the reactive alumina content in the alkali activation of fly ashes. *Microporous Mesoporous Mater* 91:111–119. <https://doi.org/10.1016/j.micromeso.2005.11.015>
- Hao D, Akatsu T, Kamochi N et al (2022) Near-zero sintering shrinkage in pottery with wollastonite addition. *J Eur Ceram Soc*. <https://doi.org/10.1016/j.jeurceramsoc.2022.10.037>
- Huseien GF, Sam ARM, Shah KW et al (2019) Evaluation of alkali-activated mortars containing high volume waste ceramic powder and fly ash replacing GBFS. *Constr Build Mater* 210:78–97. <https://doi.org/10.1016/j.conbuildmat.2019.03.194>
- Huseien GF, Sam ARM, Shah KW, Mirza J (2020) Effects of ceramic tile powder waste on properties of self-compacted alkali activated concrete. *Constr Build Mater* 236:117574. <https://doi.org/10.1016/j.conbuildmat.2019.117574>
- Ismail İ, Bernal SA, Provis JL et al (2014) Modification of phase evolution in alkali-activated blast furnace slag by the incorporation of fly ash. *Cem Concr Compos* 45:125–135. <https://doi.org/10.1016/j.cemconcomp.2013.09.006>
- Jeyasehar CA, Saravanan G, Ramakrishnan AK, Kandasamy S (2013) Strength and durability studies on fly ash based geopolymer bricks. *Asian J Civil Eng* 14:797–808
- Kaplan G, Gültekin AB (2010) The investigation of fly ash usage in terms of environmental and social effects in construction sector. Presented at the international sustainable building symposium, Ankara, pp 1–8
- Kaya M (2020) Investigation of physical and mechanical properties of geopolymer mortars produced with high and low calcium content fly ash. *Turk J Nat Sci* 9:96–104. <https://doi.org/10.46810/tdfd.782054>
- Keppert M, Vejmelková E, Bezdicka P et al (2018) Red-clay ceramic powders as geopolymer precursors: consideration of amorphous portion and CaO content. *Appl Clay Sci* 161:82–89. <https://doi.org/10.1016/j.clay.2018.04.019>
- Khale D, Chaudhary R (2007) Mechanism of geopolymerization and factors influencing its development: a review. *J Mater Sci* 42:729–746. <https://doi.org/10.1007/s10853-006-0401-4>
- Lahoti M, Yang EH, Tan KH (2017) Influence of mix design parameters on geopolymer mechanical properties and microstructure. *Ceram Eng Sci Proc* 37:21–33. <https://doi.org/10.1002/9781119321811.ch3>
- Lee Y, Kang S (2016) Effect of the CaO content on microstructure and mechanical strength of fly ash-based geopolymer. *Contem Eng Sci* 9:1413–1424. <https://doi.org/10.12988/ces.2016.69158>
- Liew YM, Heah CY, Li L et al (2017) Formation of one-part-mixing geopolymers and geopolymer ceramics from geopolymer powder. *Const Build Mater* 156:9–18. <https://doi.org/10.1016/j.conbuildmat.2017.08.110>
- Maras MM (2021) Tensile and CS strength cracking behavior of geopolymer composite reinforced with hybrid fibers. *Arab J Geosci* 14:2258. <https://doi.org/10.1016/j.conbuildmat.2018.07.012>
- Mucsi G, Szabo R, Racz A et al (2019) Combined utilization of red mud and mechanically activated fly ash in geopolymers. *Min Geol Pet Eng Bull* 34:27–36. <https://doi.org/10.17794/rgn.2019.1.3>
- Ozer İ, Soyer-Uzun S (2015) Relations between the structural characteristics and compressive strength in metakaolin based geopolymers with different molar Si/Al ratios. *Ceram Int* 41:10192–10198. <https://doi.org/10.1016/j.ceramint.2015.04.125>
- Pangdaeng S, Phoo-ngernkham T, Sata V, Chindaprasirt P (2014) Influence of curing conditions on properties of high calcium fly ash geopolymer containing Portland cement as additive. *Mater Des* 53:269–274. <https://doi.org/10.1016/j.matdes.2013.07.018>
- Peyne J, Gautron J, Doudeau J et al (2017) Influence of calcium addition on calcined brick clay based geopolymers: a thermal and FTIR spectroscopy study. *Const Build Mater* 152:794–803. <https://doi.org/10.1016/j.conbuildmat.2017.07.047>
- Pimraksa K, Hanjitsuwan S, Chindaprasirt P (2009) Synthesis of belite cement from lignite fly ash. *Ceram Int* 35:2415–2425. <https://doi.org/10.1016/j.ceramint.2009.02.006>
- Qaidi SMA, Tayeh B, Isleem HF et al (2022) Sustainable utilization of red mud waste (bauxite residue) and slag for the production of geopolymer composites: a review. *Case Stud Const Mater* 16:e00994. <https://doi.org/10.1016/j.cscm.2022.e00994>
- Qian J, Song M (2015) Study on influence of limestone powder on the fresh and hardened properties of early age metakaolin based geopolymer. In: *Calcined clays for sustainable concrete*, pp 253–259. https://doi.org/10.1007/978-94-017-9939-3_31
- Reig L, Soriano L, Borrachero MW et al (2014) Influence of the activator concentration and calcium hydroxide addition on the properties of alkali-activated porcelain stoneware. *Const Build Mater* 68:214–222. <https://doi.org/10.1016/j.conbuildmat.2014.04.023>
- Robayo-Salazar RA, de Gutiérrez RM (2018) Natural volcanic pozzolans as an available raw material for alkali-activated materials in the foreseeable future: a review. *Constr Build Mater* 189:109–118. <https://doi.org/10.1016/j.conbuildmat.2018.08.174>
- Sarıdemir M, Çelikten S, Çiftlikli M, Karahançer M (2020) Influence of calcined diatomite content and elevated temperatures on the properties of high strength mortars produced with basalt sand. *Struct Concr* 22:1–18. <https://doi.org/10.1002/suco.202000063>
- Shilar FA, Gnachari SV, Patil VB et al (2022) Evaluation of the effect of granite waste powder by varying the molarity of activator on the mechanical properties of ground granulated blast-furnace slag-based geopolymer concrete. *Polymers* 14:306. <https://doi.org/10.3390/polym14020306>



- Temuujin J, van Riessen A, Williams R (2009) Influence of calcium compounds on the mechanical properties of fly ash geopolymer pastes. *J Hazard Mater* 167:82–88. <https://doi.org/10.1016/j.jhazmat.2008.12.121>
- Thockhom S, Ghosh P, Ghosh S (2009) Effect of water absorption, porosity and sorptivity on durability of geopolymer mortars. *ARNP J Eng Appl Sci* 47:28–32
- Timakul P, Rattanaprasit W, Aungkavattana P (2016) Improving compressive strength of flyash-based geopolymer composites by basalt fibers addition. *Ceram Int* 42:6288–6295. <https://doi.org/10.1016/j.ceramint.2016.01.014>
- TS EN 1008 (2003) Mixing water for concrete—specifications for sampling, testing and assessing the suitability of water, including water recovered from processes in the concrete industry, as mixing water for concrete, Ankara, Turkey
- TS EN 1015-3 (2000a) Methods of test for mortar for masonry: Part 3. Determination of consistence of fresh mortar (by flow table) Ankara, Turkey
- TS EN 1015-11 (2000b) Mortar testing method. Part 11: measurement of compressive and flexural tensile strength of mortar TSE, Ankara, Turkey
- TS EN 1097-6 (2002) Tests for mechanical and physical properties of aggregates—part 6: determination of particle density and water absorption, Ankara, Turkey
- Vafaei M, Allahverdi A (2006) Influence of calcium aluminate cement on geopolymerization of natural puzzolan. *Constr Build Mater* 114:290–296. <https://doi.org/10.1016/j.conbuildmat.2016.03.204>
- Yip CK, Provis JL, Lukey GC, Deventer JSJ (2008) Carbonate mineral addition to metakaolin-based geopolymers. *Cem Concr Compos* 30:979–985. <https://doi.org/10.1016/j.cemconcomp.2008.07.004>
- Zeybek O (2009) Fly ash based geopolymer brick production: Master of Science thesis. Anadolu University, Turkey

Springer Nature or its licensor (e.g. a society or other partner) holds exclusive rights to this article under a publishing agreement with the author(s) or other rightsholder(s); author self-archiving of the accepted manuscript version of this article is solely governed by the terms of such publishing agreement and applicable law.

